

Contributed to the 2011 Particle Accelerator Conference, New York, N.Y., March 28 – April 1, 2011

## A LASER-DRIVEN LINEAR COLLIDER: SAMPLE MACHINE PARAMETERS AND CONFIGURATION\*

E. R. Colby<sup>#</sup>, R. J. England, R. J. Noble, SLAC, Menlo Park, CA 94025, U.S.A.

### Abstract

We present a design concept for an  $e^+e^-$  linear collider based on laser-driven dielectric accelerator structures, and discuss technical issues that must be addressed to realize such a concept. With a pulse structure that is quasi-CW, dielectric laser accelerators potentially offer reduced beamstrahlung and pair production, reduced event pileup, and much cleaner environment for high energy physics and. For multi-TeV colliders, these advantages become significant.

### MOTIVATION

With very high electric field gradients demonstrated on dielectric surfaces in narrowband (2 GV/m) [1,2] and broadband (13 GV/m) [3] cases, the use of dielectric structures for high-gradient acceleration is very attractive. The existence of 30% efficient laser sources operating in the near-IR [4] and high-quality, low-cost fabrication techniques for semiconductors [5,6] and fibers [7] motivates R&D to determine whether a usable high-energy laser-driven dielectric-structure based accelerator is feasible.

While ionization thresholds and material damage will limit a “solid-state” laser-driven accelerator to gradients well below their plasma-wakefield counterparts, what is lost in gradient is made up for in stability, efficiency, and in the potential benefits for a high-energy linear collider. Moreover, dielectric structures provide very high coupling efficiency to the beam, requiring peak powers of kilowatts—rather than terawatts—to generate GV/m-class gradients, a performance that is within easy reach of existing fiber laser systems used in the welding/cutting industry today.

### CONCEPT

Others have described concepts based on gratings[8], and swept laser structures[9]. Here we present a concept based on photonic band gap waveguides (PBGW) that offers the potential for high power efficiency required of a large-scale linear collider.

The basic accelerator structure is of either the PBG fiber type described by Lin[10] or the woodpile type described by Cowan[11]. In each case, the requirement to produce high gradient translates into (1) short laser pulses ( $<1$  ps) to avoid damage, and (2) short structures ( $<1$  mm, scaling as  $(\sigma_e + \sigma_l)/(1 - \beta_e)$ ) to avoid group velocity walkoff of the overlapping electron bunch (length  $\sigma_e$ ) and the laser pulse ( $\sigma_l$ ). Consequently, many structures must be used to obtain large integrated energy gains. Integrating multiple structures together on a common silicon (or silica) wafer

is possible with current semiconductor technology. A sketch of how woodpile structures could be integrated on a common 6” wafer to produce substantial energy gains is shown in figure 1. Three groups of PBGW structures are shown, with common fiber input and output couplers for each group of 40 structures. Such an accelerator, operating at 75% of the known damage threshold for bulk silica, would produce 130 MeV of acceleration in 15 cm, corresponding to an average gradient of 860 MeV/m.

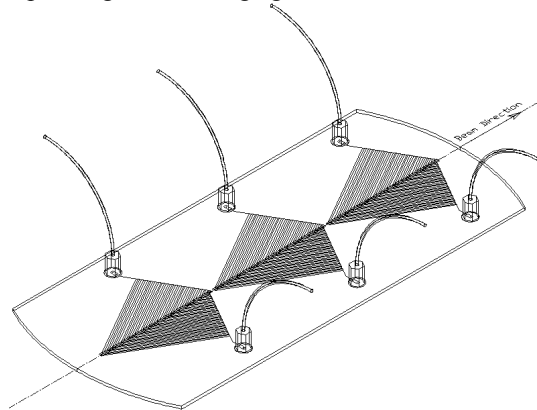


Figure 1. Concept for a laser-driven PBGW accelerator module fabricated on a single 6 inch wafer. See text.

Fiber-to-surface waveguide transitions, power splitters, and waveguides are common photonic components. The TE-to-TM PBGW couplers are the subject of current R&D, and are presented elsewhere[7,12].

Work to design laser-driven focusing structures that can be fabricated alongside the accelerator structures and powered from the same input waveguide network is underway. Early concepts were explored by Cowan, and are under development by Soong[13]. Fabricating the focusing elements in this way also ensures that alignment tolerances with respect to the surrounding structures can be held very closely—30nm or better is possible with present semiconductor techniques.

As the woodpile structure is an open lattice, it cannot sustain vacuum by itself. The structures require an external vacuum enclosure, which also serves to capture the wakefield radiation emitted from the structure. Studies of thermal and vibration effects on these structures are underway[14] and indicate that the stabilization and temperature control required are achievable.

### BEAM PARAMETERS

Reducing the accelerating wavelength by four orders of magnitude from the familiar microwave case drives many of the challenges associated with so-called Dielectric Laser Acceleration (DLA). As is obvious, this requires a

\*Work supported by DE-AC02-76SF00515 (SLAC) and DE-FG06-97ER41276.

<sup>#</sup>ecolby@slac.stanford.edu

reduction in charge and an increase in beam quality to match to the acceptance of the micron-scale apertures.

### Bunch Charge

A high-energy linear collider must generate MW-class beam powers to have sufficient luminosity for physics. Consequently, power efficiency is paramount. Efficient operation of an accelerator requires operating at the optimum bunch charge—a condition defined by [15]:

$$q_{opt} = \frac{G_0}{2\left(\frac{cZ_H}{\lambda^2} + \frac{\beta_g}{4(1-\beta_g)} \frac{cZ_C}{\lambda^2}\right)}$$

which depends on the unloaded gradient  $G_0$ , Cerenkov impedance  $Z_H$ , and accelerating mode impedance  $Z_C$  and group velocity  $\beta_g$  at wavelength  $\lambda$ . For waveguiding structures of the type discussed by Lin and Cowan, the optimum charges are  $\sim 10^6$  e/pulse and  $\sim 10^5$  e/pulse, respectively.

The use of pulse trains to increase the accelerated charge and increase the extracted power efficiency per laser pulse were examined by Siemann[15] and Cowan. Clearly, the reduction in single-bunch charge eases wakefield-driven emittance growth, but comes with a trade-off that later pulses in the train see progressively loaded gradients, increasing the energy spread. Recirculation of the laser pulse to accelerate more than one electron pulse train was also considered[16], and found to be an important way to increase the laser-to-beam coupling efficiency into the tens of percent range.

### Alignment Tolerances

Beam breakup limitations (BBU) pose strict limits on bunch charge and alignment tolerances. To estimate BBU limitations, a 3D tracking code was written, following the Chao two-particle method [17]. Initial evaluation of BBU effects has been done assuming the photonic band gap (PBG) waveguide is replaced by an annular dielectric with inner and outer radii equal to the defect radius and cladding radius, respectively, of the PBG waveguide. This yields a conservative estimate of the upper bound on the charge and alignment tolerances as the long-range wakefields of the annular dielectric are much stronger than the PBG waveguide.

Simulations show that at the optimum bunch charge of  $6 \times 10^5$  e/pulse, the BBU-induced emittance growth is consistent with the requirement to maintain the (normalized) emittance below 1 nm. Predictably, the primary driver of emittance growth is misalignment of quadrupoles in the focusing channel. Alignment tolerances for the quads of 50 nm, injection position offset of 50 nm, and injection offset angle of 75 nrad, are the tightest tolerances. While achieving such tolerances for a machine that is a few kilometres in scale is a distinct challenge, such stabilization is already demonstrated by the Seismic Attenuation System at the LIGO facility,

which has achieved better than 1 nm/ $\sqrt{\text{Hz}}$  stability at 1 Hz[18].

Further work to explore alternate focusing lattices and the introduction of BNS damping to loosen the alignment tolerances will be made.

### Emittance

Beam transport through the micron-scale accelerator aperture places stringent limits on the emittance. The acceptance of a channel of radius  $r$  with optical function maximum  $\beta_{max}$  is  $A=r^2/\beta_{max}=n^2\varepsilon/\gamma$ , where  $n=r/\sigma$ , and  $\sigma$  is the rms beam size. Given quadrupoles of gradient  $K$ , length  $l$ , and a lattice phase advance of  $\phi$ , the requirement on the normalized emittance reads:

$$\varepsilon < \frac{r^2}{n^2} \frac{eKl}{2mc} \frac{\cos\phi}{1 + \sin\phi}$$

We consider two cases: conventional focusing using permanent magnet quadrupoles and integrated focusing, and PBG waveguiding structures designed to produce focusing fields. For the conventional case,  $r \sim 2 \mu\text{m}$ ,  $K \sim 2.5$  kT/m,  $l \sim 1$  cm and a stay-clear safety factor of  $n=5$ , requires the emittance  $\varepsilon < 0.3$  nm. For integrated focusing, gradients of up to 1 MT/m are consistent with damage thresholds of the materials; taking  $K \sim 100$  kT/m,  $l=1$  mm, requires the emittance  $\varepsilon < 1.3$  nm, relaxing the emittance requirement by a factor of  $\sim 4$  and shortening the focusing elements by a factor of ten.

While at first inspection such a small emittance appears problematic, the phase space density  $N/\varepsilon \sim 10^5/10^{-9} \sim 10^{14}$   $\text{m}^{-1}$  is lower than has been achieved at the LCLS ( $N/\varepsilon \sim 10^9/10^{-7} \sim 10^{16}$   $\text{m}^{-1}$ ), and is consistent with what has been produced from field-emission sources[19].

### Luminosity

Producing the required luminosity from such small bunch charges requires that both the repetition rate be raised and the spot sizes be reduced to compensate. This is indeed possible, owing to two factors.

First, the ability to raise the repetition rate significantly is a unique attribute of DLA. The use of low-peak power CW laser systems allows repetition rates in the  $10^8$  Hz range with continuous duty factor to be discussed. This is not possible with either klystron-based concepts nor very high peak power laser concepts as neither is capable of such repetition rates or duty factors.

Second, the small emittances permit smaller focused spot sizes at the IP. Ordinarily, reduction in spot size is accompanied by unwanted levels of beamstrahlung and background, but the significantly reduced bunch charges for the DLA case mitigate these problems. Furthermore, the beamstrahlung-induced energy spread at collision is also significantly reduced, which will increase the precision of the physics.

We combine these considerations to provide an illustrative comparison of linear collider schemes scaled to 3 TeV c.o.m. energy and a luminosity  $L=9 \times 10^{34}$   $\text{cm}^{-2}\text{s}^{-1}$

in Table 1. Immediately noticeable are the substantial beamstrahlung and pair production rates for the klystron-driven cases of ILC, CLIC, and plasma wakefield. The much smaller bunch charges of the DLA suffer little

induced energy spread ( $\Delta p/p$  beamstrahlung) or pair production, leading to a substantially cleaner environment for particle physics.

**Table 1: Illustrative parameters of several linear collider schemes at 3 TeV**

Parameter	Units	"ILC"	"CLIC"	Plasma Wake	DLA 2 micron	DLA 4 micron
$E_{cm}$	GeV	3000	3000	3000	3000	3000
$\gamma$		2.94E+06	2.94E+06	2.94E+06	2.94E+06	2.94E+06
Accel Wavelength	cm	23.1	2.5	0.01	0.0002	0.0004
N		1.7E+10	2.9E+09	9E+08	3216	12864
nb		3400	312	2100	145	145
Tsep	ns	205.8824	0.5	40	6.67E-06	1.33E-05
$I_{ave}$ in 1 second	$\mu A$	46.3	7.3	18.2	13.1	6.6
Repetition Rate	Hz	5	50	60	175 MHz	22 MHz
$P_b$ one beam	MW	69.4	10.9	27.3	19.6	9.9
<b>IP Parameters</b>						
$\gamma \epsilon_x$	m	0.00001	6.6E-07	0.000001	1E-10	1E-10
$\gamma \epsilon_y$	m	4E-08	2E-08	1E-09	1E-10	1E-10
$\beta_x$	m	0.03	0.004	0.01	0.0001	0.0002
$\beta_y$	m	0.0003	0.00007	0.0002	0.0001	0.0002
$\sigma_x$ geometric	m	3.2E-07	3E-08	5.84E-08	5.84E-11	8.25E-11
$\sigma_y$ geometric	m	2.02E-09	6.91E-10	2.61E-10	5.84E-11	8.25E-11
$\Delta p/p$ (beamstrahlung)	%	17%	42%	7%	5.20E-07	2.07E-06
$P_{Beamstrahlung}$	MW	11.68	4.51	1.95	1.02E-02	2.04E-05
$n\gamma$		1.84	1.83	0.36	1.21E-03	3.42E-03
$H_d$		1.49	1.78	1.70	1.00	1.01
Geom Luminosity	$m^{-2} s^{-1}$	6.0E+38	5.0E+38	5.3E+38	8.9E+38	8.9E+38
Enh. Luminosity	$m^{-2} s^{-1}$	8.99E+38	8.98E+38	9.04E+38	8.89E+38	9.01E+38
Coherent pairs	1/bx	1.09E+04	2.14E+08	9.13E+05	0.00E+00	0.00E+00
Inc. Pairs (total)	1/bx	9.25E+05	7.51E+05	3.87E+04	1.22E-01	1.00E+00
Active Linac Length	km	85.7	30.0	0.3	3.5	3.5

## CHALLENGES AND NEXT STEPS

The next steps towards demonstrating the potential of DLA are to prepare components and experimentally demonstrate:

- High gradient potential (>200 MV/m)
- High integrated energy gain (>20 MeV)
- Integration of focusing and diagnostics
- High power transfer efficiency
- Stable transport through meters of accelerator

Further work to examine focusing lattices that raise the BBU limits on bunch charge will benefit all applications of this technology.

Although methods for generating electron beams of the required brightness exists, there are no known methods for generating positron beams of the required brightness.

## ACKNOWLEDGEMENTS

We thank Tor Raubenheimer for discussions of linear collider design issues, and Andrei Seryi for providing his

LC parameter worksheet, and for checking the analytic estimates of the disruption parameter with Guinea Pig.

## REFERENCES

- [1] B. Stuart, *Phys. Rev. Lett.*, **74**, p. 2248, (1995).
- [2] K. Soong, MOP071, in these proceedings, (2011).
- [3] M. Thompson, *Phys. Rev. Lett.*, **100**, 214801, (2008).
- [4] <http://www.ipgphotonics.com>.
- [5] C. McGuinness, *J. Mod. Opt.*, **56**, p. 2142, (2009).
- [6] C. McGuinness, MOP133, these proceedings, (2011).
- [7] J. Spencer, MOP136, in these proceedings (2011).
- [8] R. Palmer, *Part. Accel.*, **11**, p81ff, (1980).
- [9] A. Mikhailichenko, proc. PAC'99, p. 3633ff, (1999).
- [10] X. E. Lin, *PRST-AB*, **4**, 051301 (2001).
- [11] B. Cowan, *PRST-AB*, **11**, 011301 (2008).
- [12] Z. Wu, MOP072, in these proceedings (2011).
- [13] K. Soong, MOP104, in these proceedings (2011).
- [14] R. Laouar, TUP276 in these proceedings, (2011).
- [15] R. Siemann, *PRST-AB*, **7**, 061301 (2004).
- [16] R. Siemann, *PRST-AB*, **8**, 031301 (2005).

- [17] A. Chao, *Physics of Collective Beam Instabilities in High Energy Accelerators*, John Wiley&Sons, 1993.
- [18] A. Sochino, *NIM-PRA*, **598**, p. 737ff (2009).
- [19] P. Hommelhoff, *Phys. Rev. Lett.*, **96**, 077401 (2006).